

Marburg virus RNA synthesis is inhibited by a synthetic anti-VP35 antibody

Parmeshwar Amatya^{1*}, Nicole Wagner^{2*}, Gang Chen^{3*}, Priya Luthra⁴, Liuqing Shi², Dominika Borek⁵, Alevtina Pavlenco³, Henry Rohrs², Christopher F. Basler⁴, Sachdev S. Sidhu^{3#}, Michael L. Gross^{2#}, and Daisy W. Leung^{1,6#}

Supporting Information:

Supporting Figure Legends

Table S1. Data collection and refinement statistics.

Figure S1. Peptide coverage maps for mVP35 IID, sFab H3 light chain, and sFab H3 heavy chain.

Figure S2. HDX-MS heatmaps of sFab H3.

Figure S3. HDX kinetics curves of mVP35 IID peptides.

Figure S4. HDX kinetics curves of sFab H3 light chain peptides.

Figure S5. HDX kinetics curves of sFab H3 heavy chain peptides.

Figure S6. Fluorescence polarization assay measuring binding of sFab H3 to mVP35 IID with dsRNA.

Figure S7. Pull-down assay of eVP35 IID mutant binding to sFab H5.

Supporting Figure Legends

Table S1. Data collection and refinement statistics.

Figure S1. Coverage maps of all peptides acquired for **A.** mVP35 IID showing 87 peptides with 100% coverage, **B.** sFab H3 light chain showing 200 peptides with 100% coverage, and **C.** sFab H3 heavy chain showing 219 peptides with 99.6% coverage.

Figure S2. HDX-MS heatmaps of unbound **A.** sFab H3 light chain and **B.** sFab H3 heavy chain. The extent of deuteration is depicted following the included gradient bars.

Figure S3. HDX kinetics curves of all mVP35 IID peptides of every observed charge state (89 total) when (black) unbound, (red) bound to sFab H3, and (blue) bound to sFab H5. Some peptides from the original mapping experiments were excluded due to low signal and/or interference. Each page contains the results for 40 peptides ordered from N-terminal to C-terminal.

Figure S4. HDX kinetics curves of all sFab H3 light chain peptides of every observed charge state (151 total) when (black) unbound and (red) bound to mVP35 IID. Each page contains the results for 40 peptides ordered from N-terminal to C-terminal.

Figure S5. HDX kinetics curves of all sFab H3 heavy chain peptides of every observed charge state (170 total) when (black) unbound and (red) bound to mVP35 IID. Each page contains the results for 40 peptides ordered from N-terminal to C-terminal.

Figure S6. mVP35 IID binds to dsRNA with similar affinity in the presence or absence of sFab H3. Fluorescence polarization assay based on the interaction of mVP35 IID to a FITC-labeled 19 bp dsRNA. 1 nM FITC-19 bp dsRNA has low fluorescence polarization across 5 samples (black squares). Addition of 100 nM mVP35 IID results in an increase in fluorescence polarization (red squares), indicating binding. Addition of 50 nM of sFab H3 to 1 nM FITC-19 bp dsRNA containing 100 nM of mVP35 IID results in a further increase in fluorescence polarization (blue squares) due

to formation of mVP35 IID-sFab H3-dsRNA complex. No increase in fluorescence polarization was observed upon addition of 50 nM sFab H3 to 1 nM FITC-dsRNA (compare green circles with cyan circles) or 100 nM maltose binding protein to 1 nM FITC-dsRNA (compare yellow triangles to pink triangles).

Figure S7. In vitro pull-down assay of eVP35 IID mutant binding to sFabs H5. Lane 1, sFab; lane 2, sFab + resin negative control; lane 3, immobilized MBP-fusion protein; lane 4, input; lanes 5-6, washes; lane 7, final bound resin; lane 8, eluate.

Table S1. Data collection and refinement statistics

Data collection	
Space Group	<i>P2₁2₁2</i>
Unit cell parameters	
<i>a</i> , <i>b</i> , <i>c</i> (Å)	57.83, 97.42, 110.33
α , β , γ (°)	90, 90, 90
Resolution range (Å) ^{1,2}	50.00-1.70 (1.73 – 1.70)
Limit along <i>a</i> *	~1.85
<i>b</i> *	~1.75
<i>c</i> *	~1.60
Unique reflections	68713 (3348)
Redundancy	6.9 (7.1)
Completeness (%)	99.4 (99.1)
Wilson B factor	
Average B, all atoms (Å ²)	20.16
<i>R</i> _{merge} (%)	12.8 (117)
$\langle I \rangle / \langle \sigma(I) \rangle$	15.8 (1.72)
<i>CC1/2 last shell</i>	(0.721)
Refinement	
Resolution (Å)	36.96 – 1.70 (1.75 – 1.70)
No. of reflections	61776 (3022)
Completeness (%)	93.83 (63.15)
Total No. of non-hydrogen atoms	5064
<i>R</i> _{work} / <i>R</i> _{free} (%)	19.58/23.30 (25.1/30.4)
R.m.s. deviations	
Bond lengths (Å)	0.006
Bond angles (°)	1.307
<i>B</i> -factors (Å ²)	
VP35 IID	27.8 (chain A)
sFab H3 heavy chain	17.1 (chain H)
sFab H3 light chain	21.2 (chain L)
water	27.8 (chain W)
Ramachandran plot outliers (%)	0.18%
Molprobity Clashscore, all atoms	2.6 (99 th percentile)
Molprobity Score	1.16 (99 th percentile)

¹Values in parentheses are for the highest resolution shell.

²Anisotropy is presented along three directions of reciprocal lattice. The anisotropy of diffraction is the reason for the ellipsoidal truncation during refinement that results in lower completeness in the highest resolution shell.

Figure S1

A

205 210 215 220 225 230 235 240 245 250 255 260 265 270 275 280 285 290 295 300 305 310 315 320 325
201GHMSKPNLSAKDLALLLFTLHPGNNTFFHILAQVLSKIAYKSGKSGAFLDAFHQILSEGENAQAALTRLRSTFDALFVGVPPVIRVKNFQTVPRPCCOKSLRAVPPNFTIDKGWVCVYSSEQGETRALKI

B

5 10 15 20 25 30 35 40 45 50 55 60 65 70 75 80 85 90 95 100 105 110 115
1DIQMT QSPSS LSASV GDRVT ITCRA SQSVS SAVAW YQOKP GKAPK LLIYS ASSLY SGVPS RPSGS RSGTD FTLTI SSLQP EDFAT YYCQQ GYYVA YSLIT FGQGT KVEIK RTVAA

120 125 130 135 140 145 150 155 160 165 170 175 180 185 190 195 200 205 210 215 220 225
116PSVFI FPPSD SQLKS GTASV VCLLN NFYPR EAKVQ WKVDN ALQSG NSQES VTEQD SKDST YLSS TLTLKADYE KHKVY ACEVT HQGLS SPVTK SFNRG ECGGS DYKDD DDK

C

8 13 18 23 28 33 38 43 48 53 58 63 68 73 78 83 88 93 98 103 108 113 118
4EVQLV ESGGG LVQPG GSLRL SCAAS GFNIS YYVYH WVRQA PGKGL ENVAS IYPYI GYTSY ADSVK GRFTI SADTS KNTAY LQMNS LRAED TAVYI CARGS SWYGA HAFDY WGQGT

123 128 133 138 143 148 153 158 163 168 173 178 183 188 193 198 203 208 213 218 223 228 233
119LVTVS SASTK GPSVF PLAPS SKSTS GGTAA LGCLV KDYFP EPVTV SWNSG ALTSG VHTFP AVLQS SGLYS LSSVV TVPSS SLGTQ TYICN VNHKP SNTKV DKKVE PKSCD KHTTS

238
234RHHHH HH

Figure S2

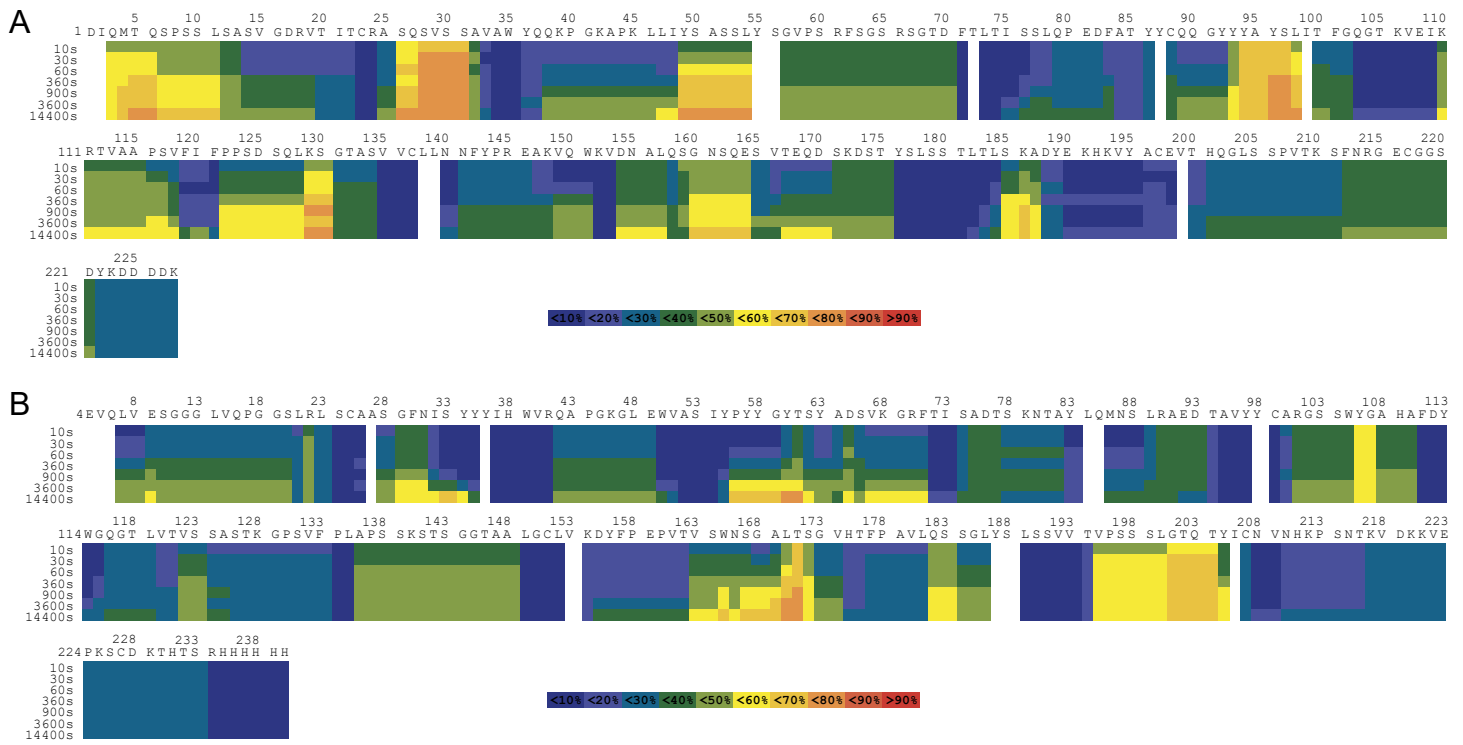
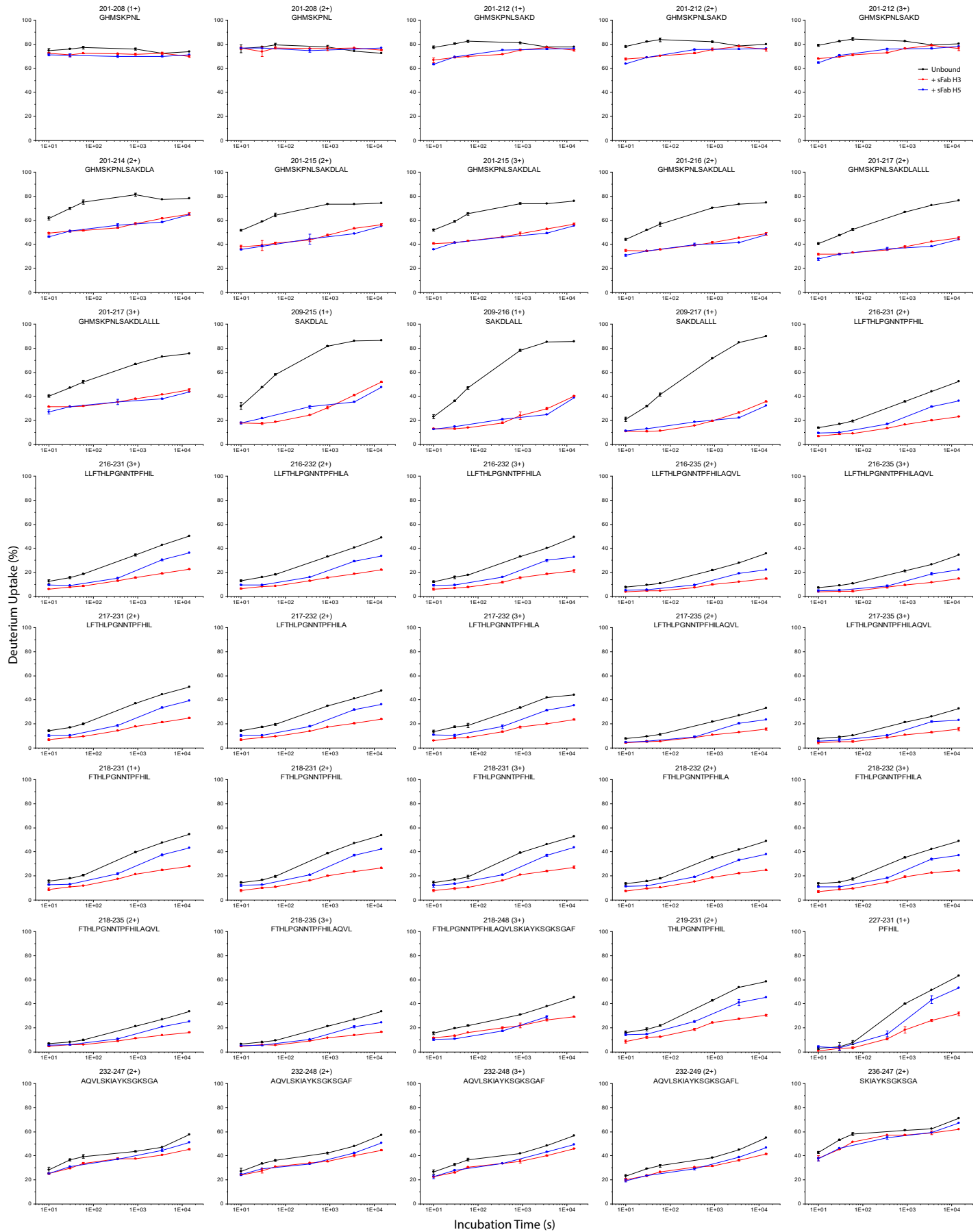
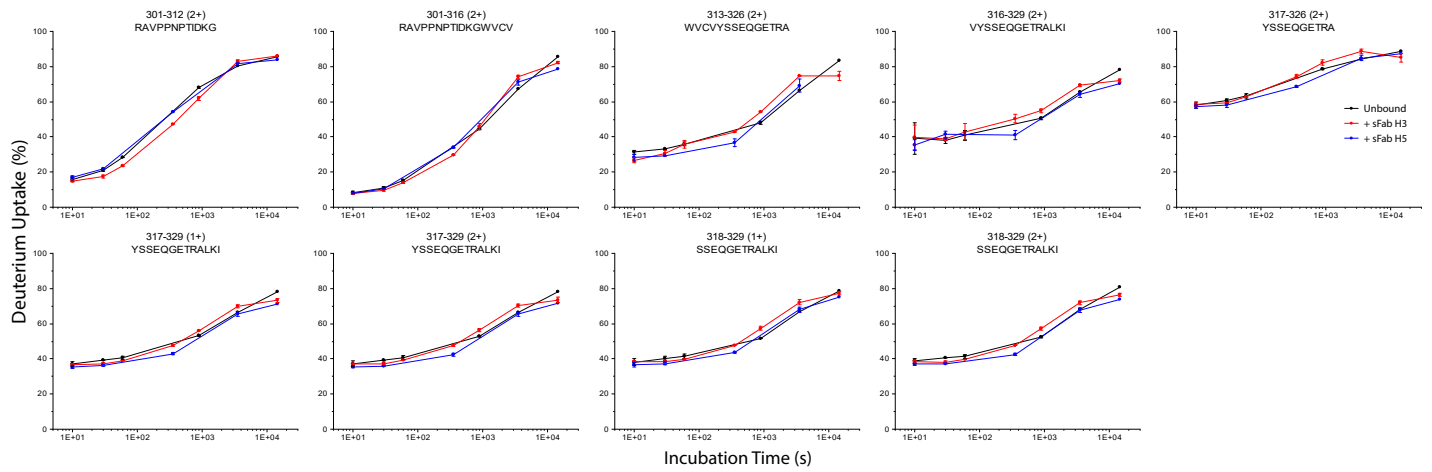


Figure S3-1. mVP35 IID



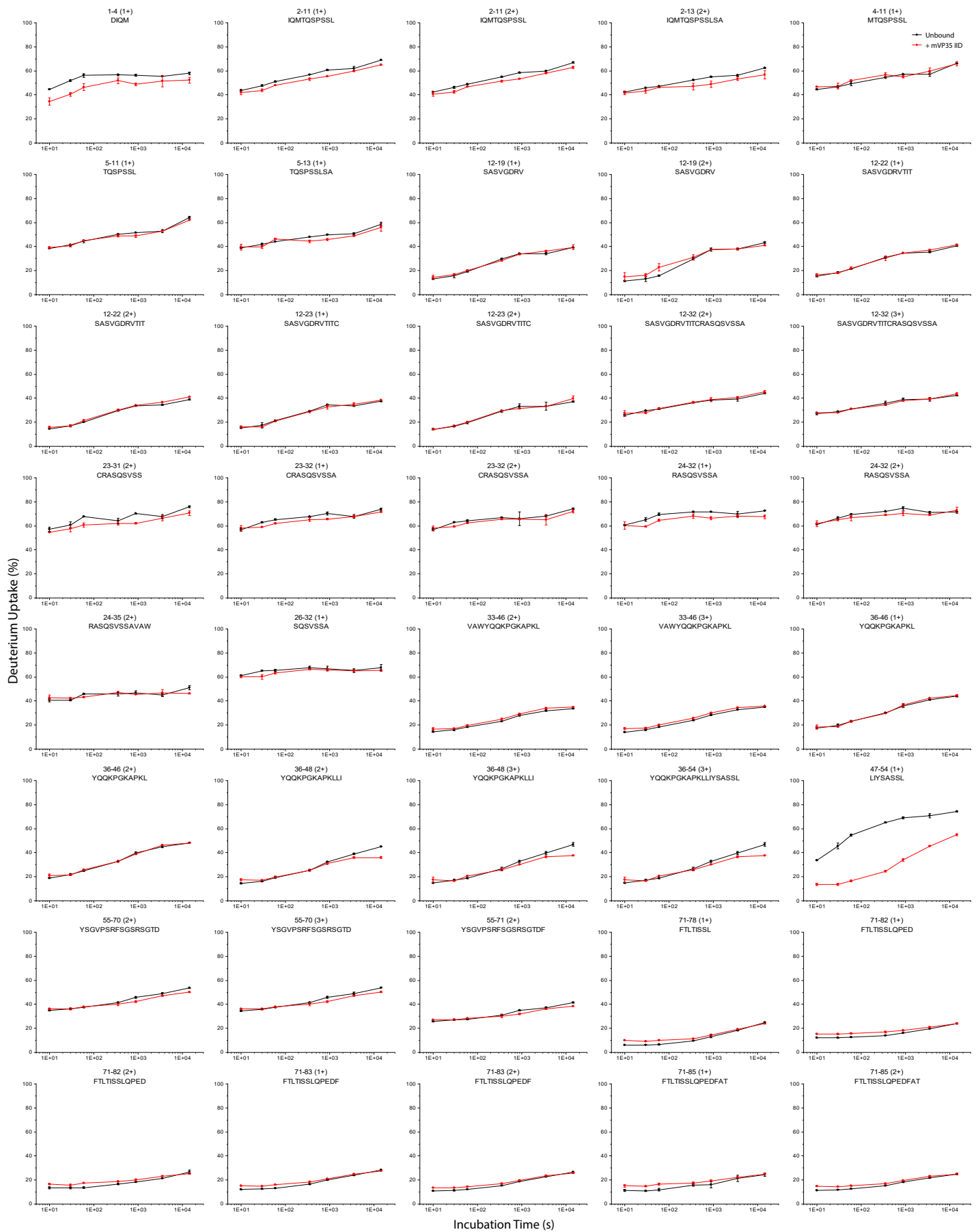
HDX kinetics curves of all mVP35 IID peptides when (black) unbound, (red) bound to Fab H3, and (blue) bound to Fab H5.

Figure S3-3. mVP35 IID



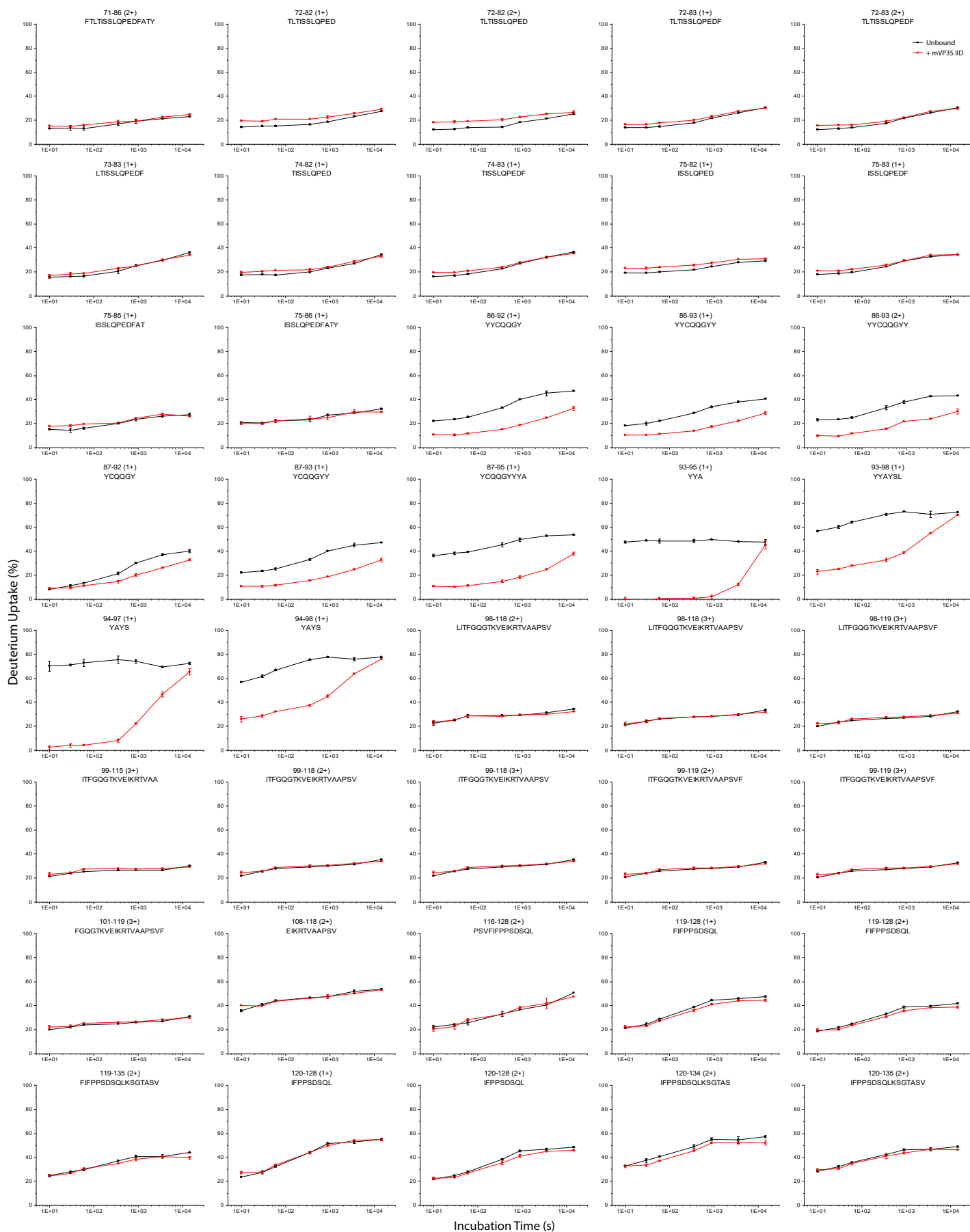
HDX kinetics curves of all mVP35 IID peptides when (black) unbound, (red) bound to Fab H3, and (blue) bound to Fab H5.

Figure S4-1. Fab H3 Light Chain



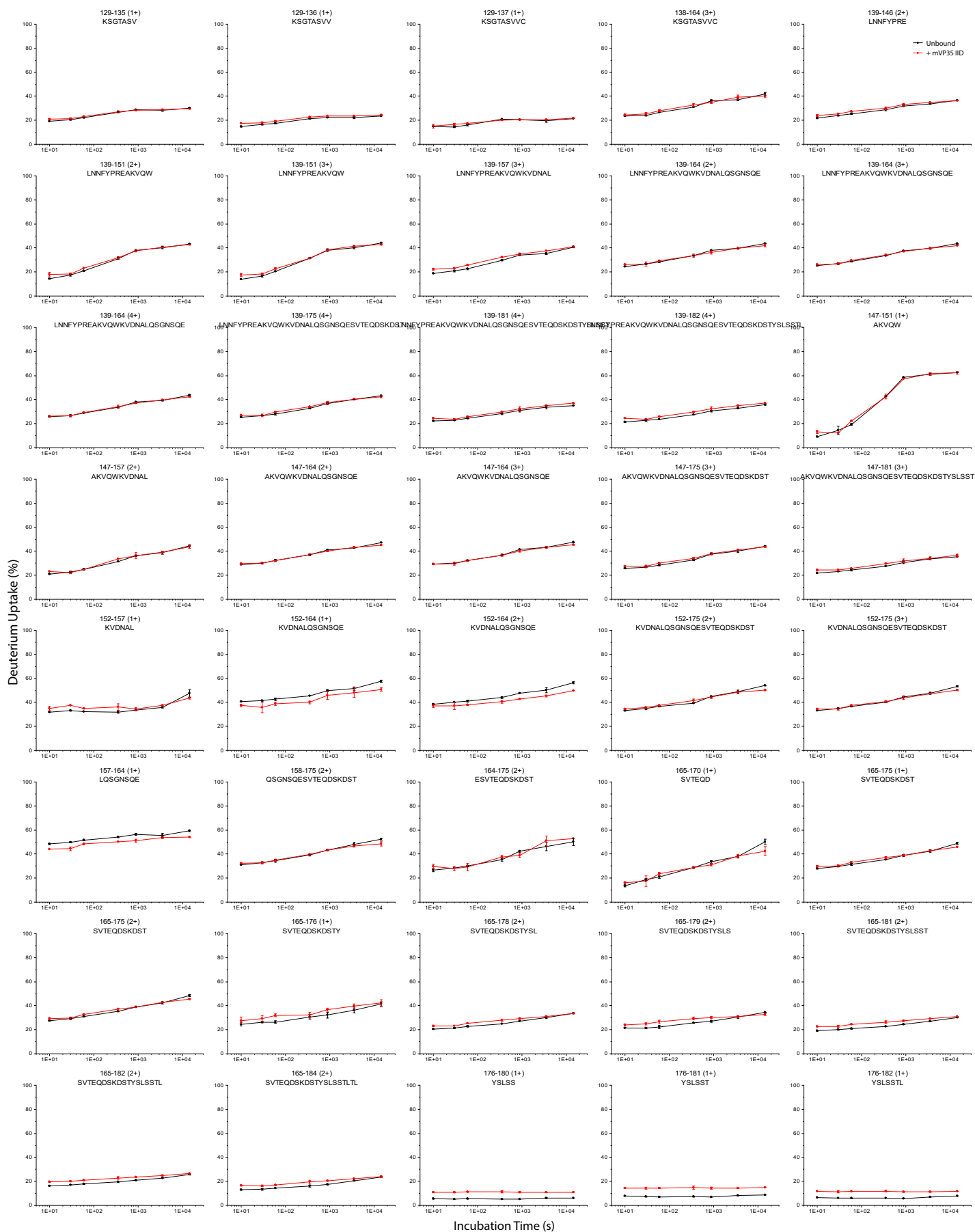
HDX kinetics curves of all Fab H3 light chain peptides when (black) unbound and (red) bound to mVP35 IID.

Figure S4-2. Fab H3 Light Chain



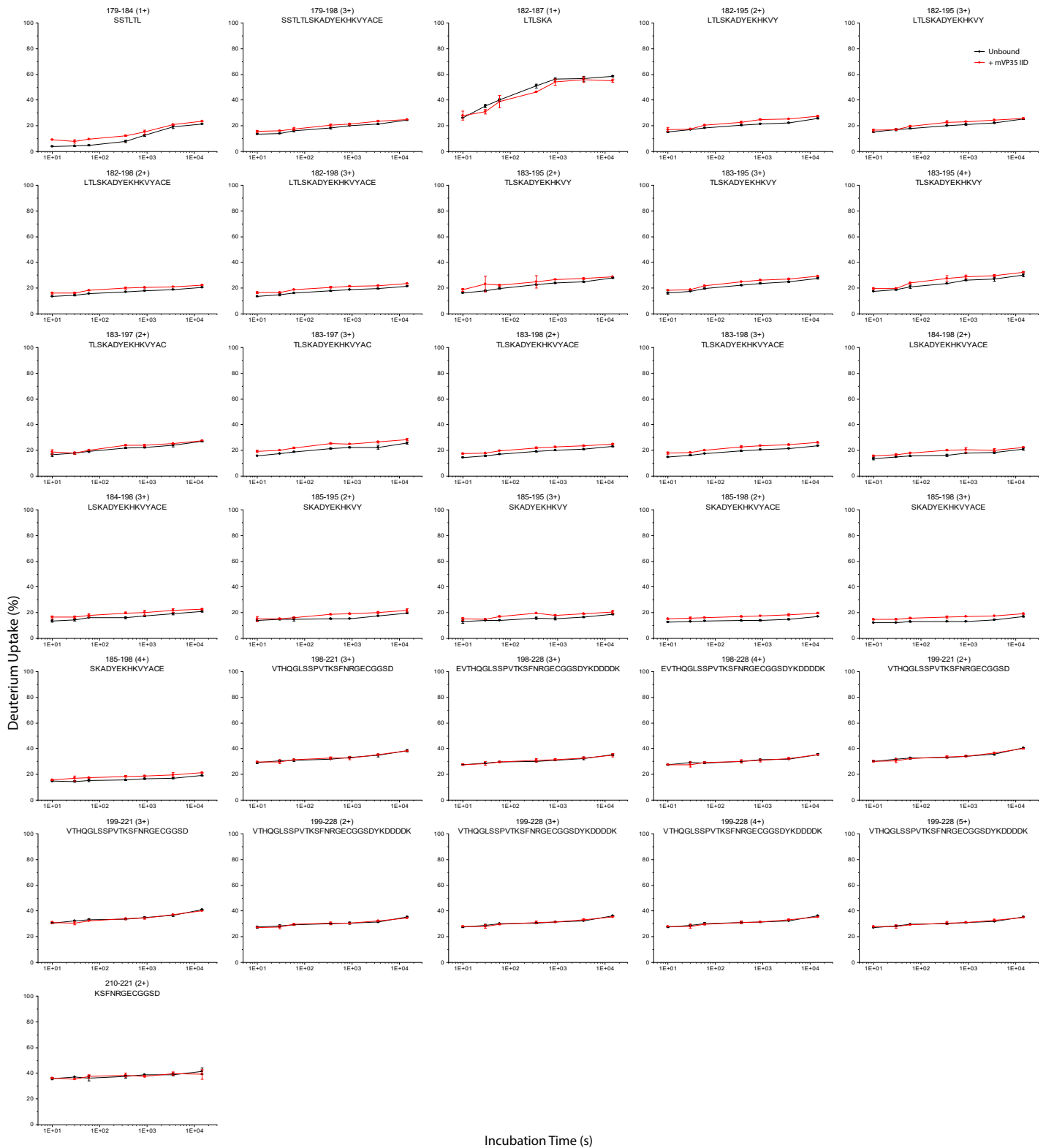
HDX kinetics curves of all Fab H3 light chain peptides when (black) unbound and (red) bound to mV35 IID.

Figure S4-3. Fab H3 Light Chain



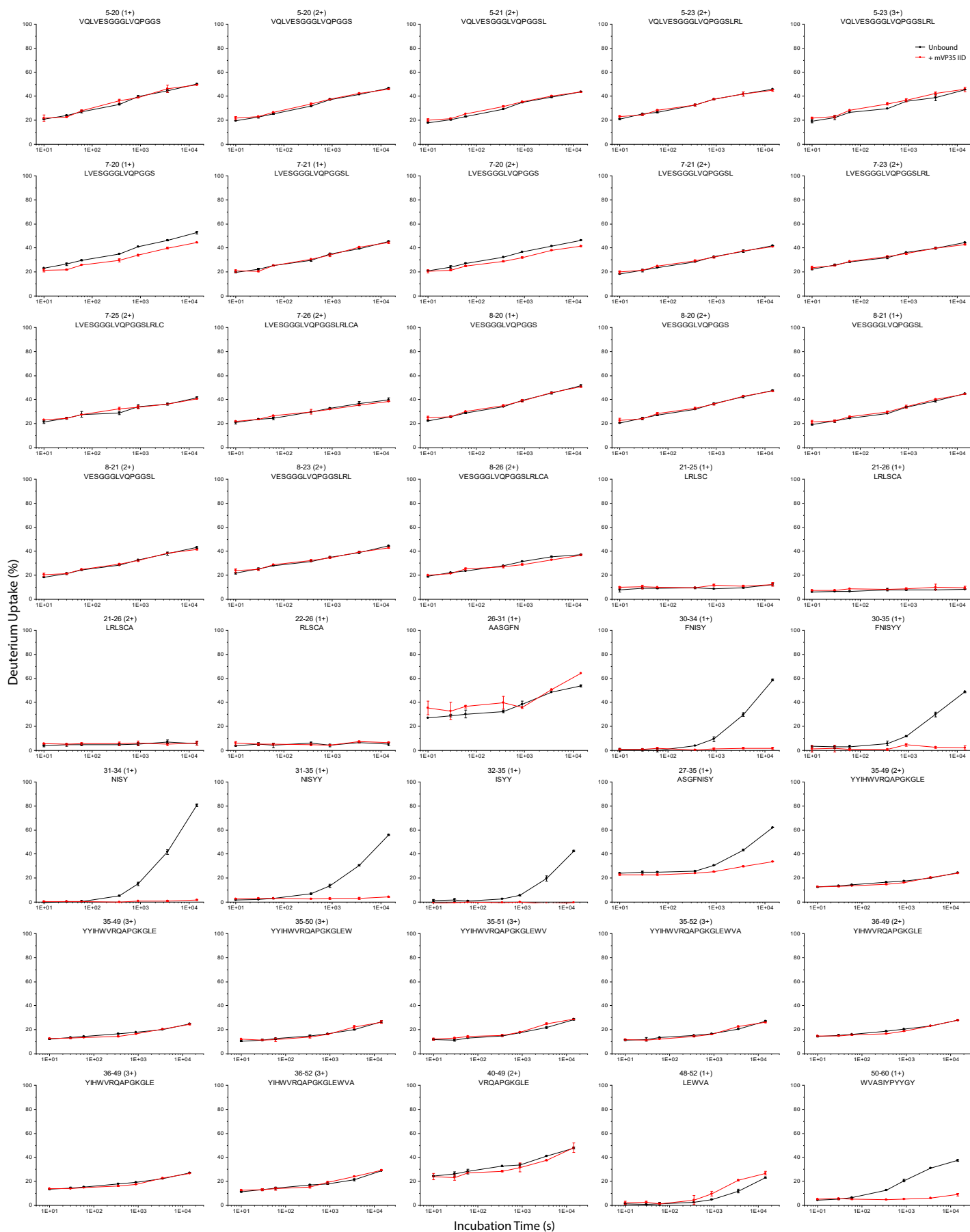
HDX kinetics curves of all Fab H3 light chain peptides when (black) unbound and (red) bound to mVp35 IID.

Figure S4-4. Fab H3 Light Chain



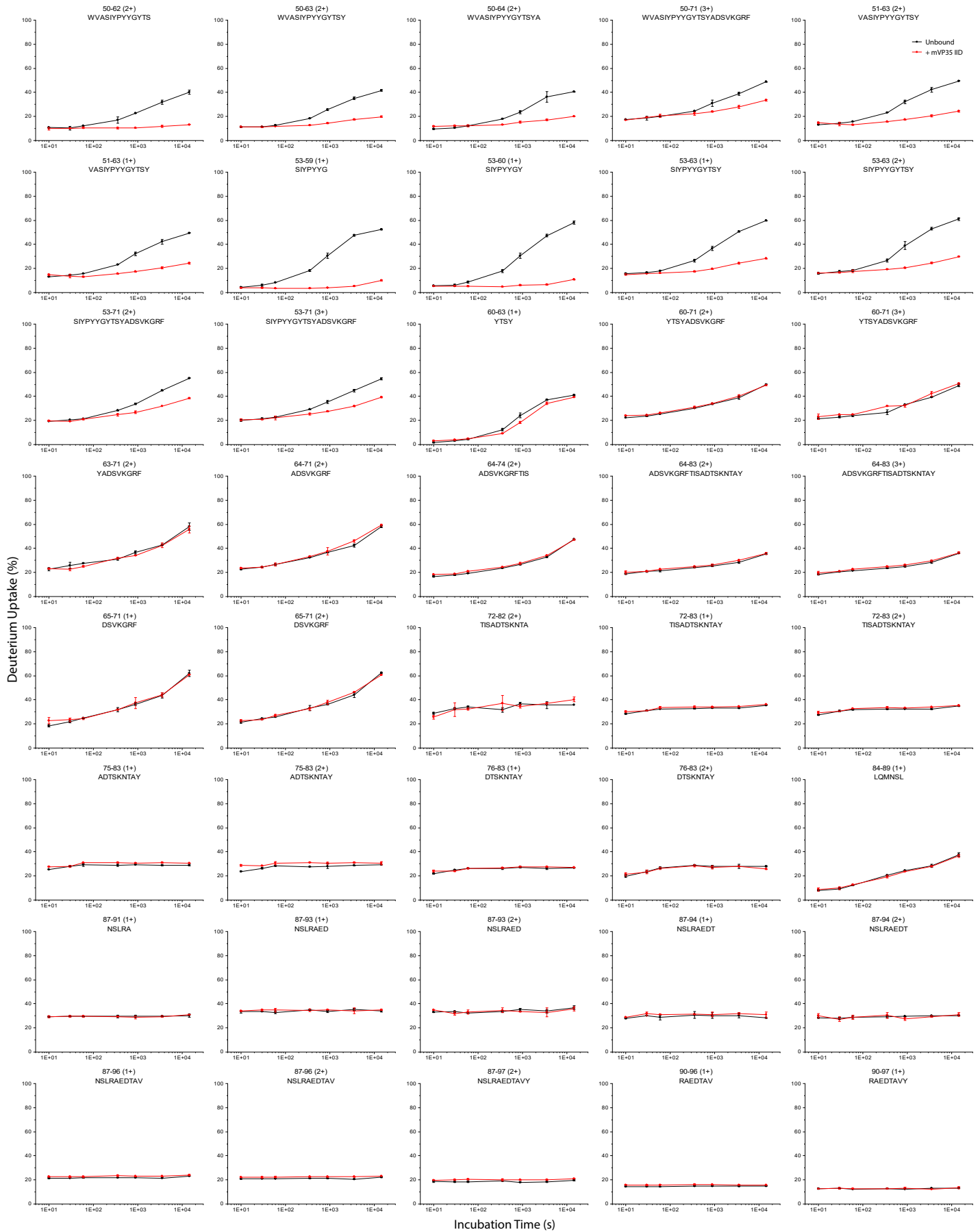
HDX kinetics curves of all Fab H3 light chain peptides when (black) unbound and (red) bound to mVP35 IID.

Figure S5-1. Fab H3 Heavy Chain



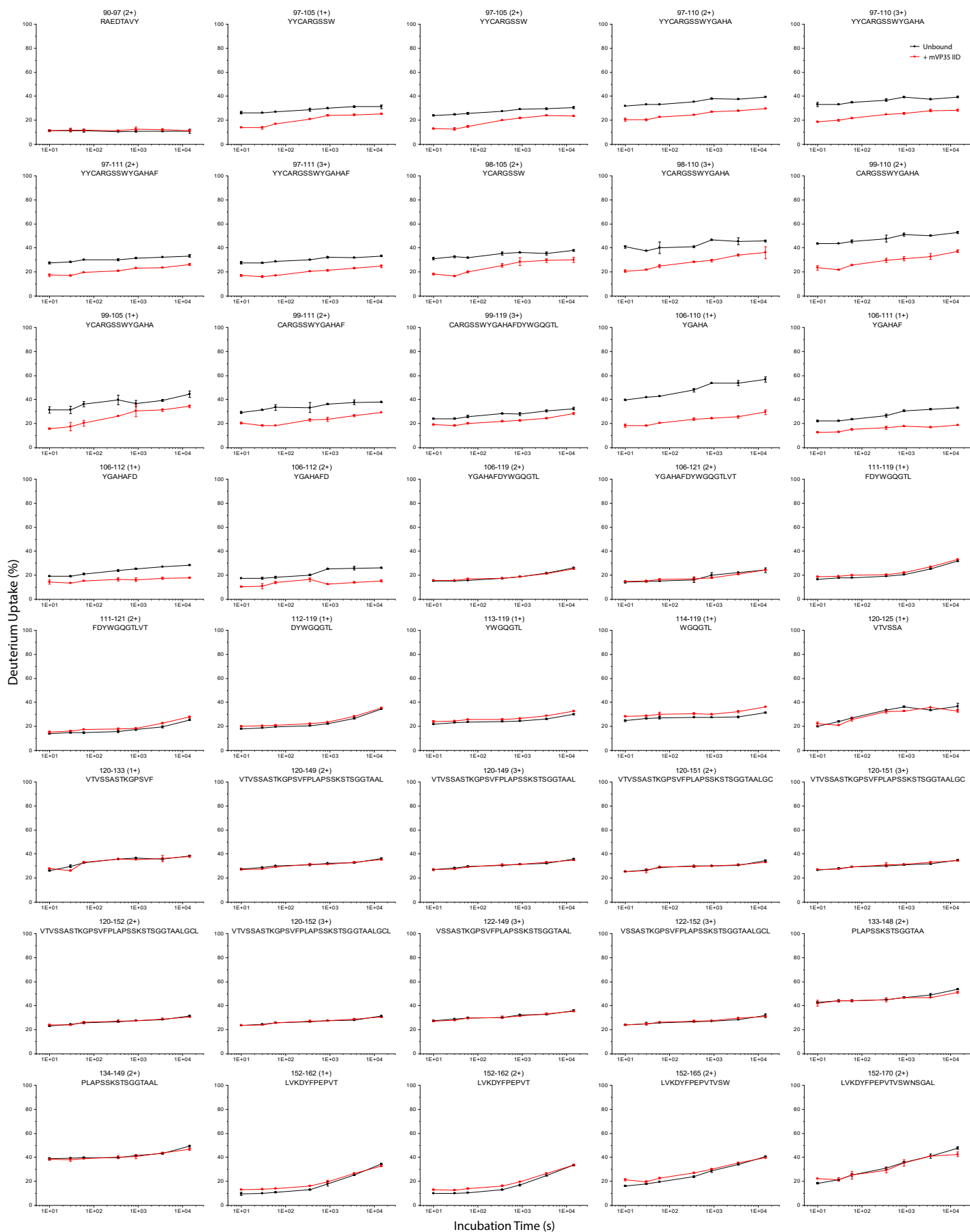
HDX kinetics curves of all Fab H3 heavy chain peptides when (black) unbound and (red) bound to mVP35 IID.

Figure S5-2. Fab H3 Heavy Chain



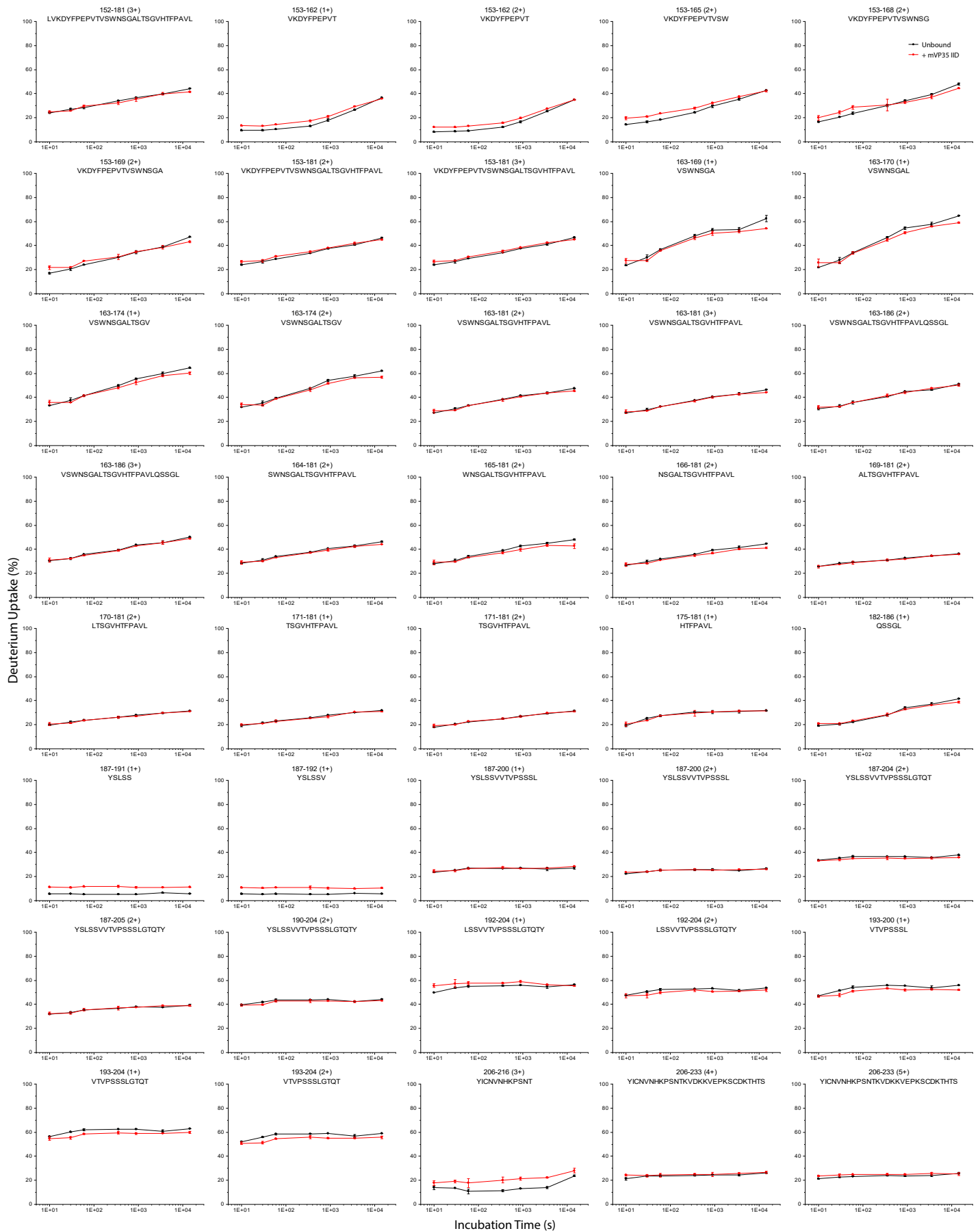
HDX kinetics curves of all Fab H3 heavy chain peptides when (black) unbound and (red) bound to mVP35 IID.

Figure S5-3. Fab H3 Heavy Chain



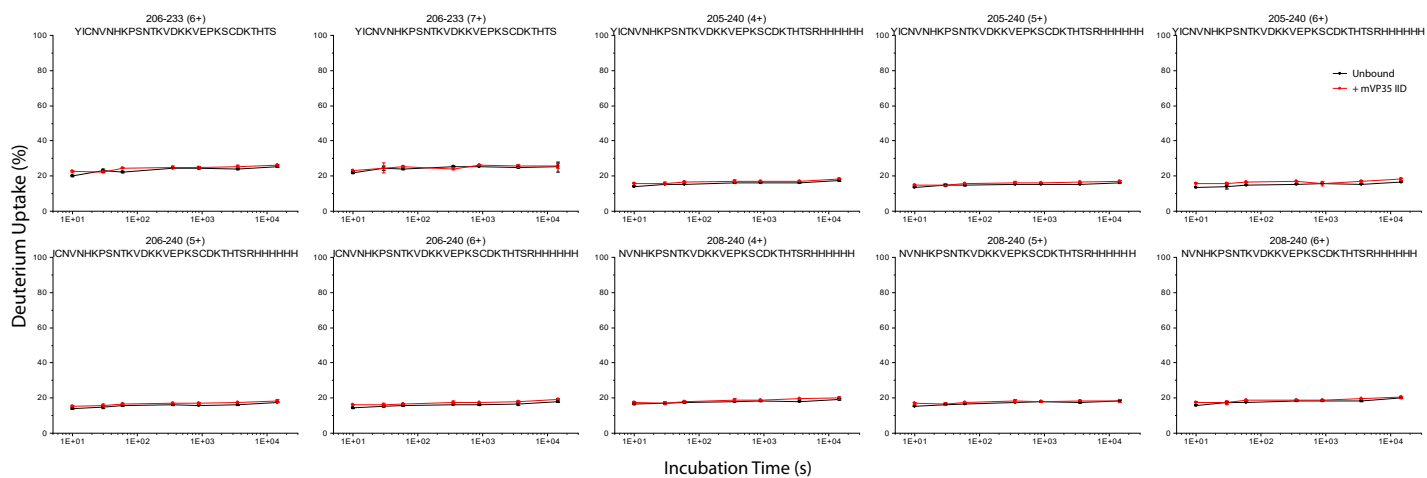
HDX kinetics curves of all Fab H3 heavy chain peptides when (black) unbound and (red) bound to mVP35 IID.

Figure S5-4. Fab H3 Heavy Chain



HDX kinetics curves of all Fab H3 heavy chain peptides when (black) unbound and (red) bound to mVP35 IID.

Figure S5-5. Fab H3 Heavy Chain



HDX kinetics curves of all Fab H3 heavy chain peptides when (black) unbound and (red) bound to mVP35 IID.

Figure S6

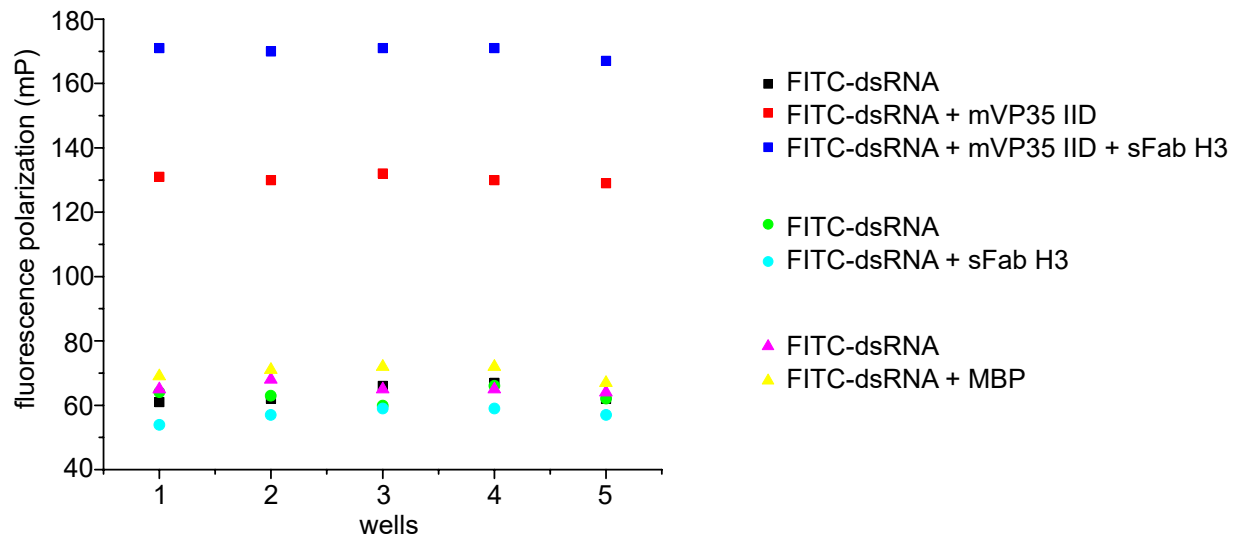


Figure S7

